Efficient Probabilistic Approach to Range-Only SLAM With a Novel Likelihood Model

Jun Wang, Ziyang Meng, *Senior Member, IEEE*, and Lei Wang

***Abstract*— The range-only simultaneous localization and mapping (RO-SLAM) problem is considered in this article. This is a difficult problem since bearing measurements are not available. Also, the frequent outliers induced by the sensor nature (typically sonar or radio pulses) render the RO-SLAM problem more challenging. The non-Gaussian distribution found in the RO-SLAM problem makes that the landmarks cannot be directly updated using the approach based on the Gaussian assumption. We propose a region-based particle filter and a proper likelihood model to realize the reduction of particle numbers and allow the introduction of new landmarks without delayed processing. A transition mode is designed from the loosely coupled way to the tightly coupled way and used to estimate the pose of the robot and locations of landmarks. Furthermore, two detection methods are, respectively, used to remove the outliers generated by the range-only sensors according to the distribution status of the landmark estimation. The proposed algorithm is evaluated through simulations and experiments with a range-only sensor, i.e., Ultrawideband (UWB). Furthermore, the obtained results are compared with the classical algorithm. The simulation and experiment results verify the validity and superiority of the proposed RO-SLAM algorithm.**

***Index Terms*— Likelihood function, particle filter, range only, simultaneous localization and mapping (SLAM), ultrawideband (UWB).**

I. Introduction

SIMULTANEOUS localization and mapping (SLAM) is one of the most important issues for autonomous mobile robots and much attention has been paid to this field in recent years. From a measurement perspective, cameras and laser range finders (LRFs) are widely used in current SLAM solutions. In contrast to LRFs and stereo cameras (both supporting range and bearing information), relatively few works address the SLAM problem with sensors providing range-only information, i.e., Ultrawideband (UWB) [1], Ultra-high frequency (UHF) band radio frequency identification (RFID) [2], despite their important applications such as submarine autonomous vehicles, ground vehicles in industrial environments, or urban search and rescue. Range-only sensors are low-power sensors that are able to provide the distance measurements between two sensors and the relative distance is quite long. One great advantage of using the sensors such as active radio or sonar beacons is that a robust data-association can be achieved because the measurements are often accompanied by the unique identity of the source of the signal.

Range-only SLAM (RO-SLAM) simultaneously localizes the mobile robot and builds the map of the landmarks equipped with the range-only sensors. The ambiguity of the range only measurements and the existence of outliers render RO-SLAM especially challenging [3], [4]. The lack of bearing information in RO-SLAM leads to uniform distributions in the location of the landmark, which makes it difficult to integrate into common Gaussian filters or graph optimization directly. The particle filter is a useful approach to fit the uniform distribution of the landmark location in the initialization stage [5]–[7]. However, the number of the particles to be generated is a crucial parameter of this approach: too few particles may lead to a wrong estimation while an excessive number increases the computational burden. One main issue with using the particle filter to initialize the landmark location is to reduce the number of particles while maintaining accuracy. The conventional particle filter method uses particles to describe the potential location of a landmark. This point-based particle filter requires a large number of particles to ensure accuracy.

In this article, we use particles to represent the potential regions of a landmark such that the number of particles can be effectively reduced. To adapt this type of particle, a proper likelihood model is proposed for the range-only sensors. This novel likelihood model also allows the introduction of new landmarks without delayed processing. A loosely coupled way is used to combine the particle filters to estimate the robot pose and landmark locations simultaneously. When the particle filter for estimating the landmark locations eventually converges to a small Gaussian-like distribution, it will be replaced by a standard extended Kalman filter (EKF) and form a tightly coupled pattern with the particle filter for estimating the robot pose. This combination of loose coupling and tight coupling reduces the computational burden and makes the proposed algorithm more robust against the outliers. Furthermore, according to the utilization of the nonparametric or parametric approaches [8] to estimate the landmark location, a hypothesis testing method and a coarse detection method are, respectively, used to further eliminate the effects of outliers on the accuracy of the RO-SLAM algorithm.

Manuscript received January 22, 2021; revised March 10, 2021; accepted March 27, 2021. Date of publication April 9, 2021; date of current version April 26, 2021. This work was supported in part by the Institute for Guo Qiang of Tsinghua University under Grant 2019GQG1023, in part by the National Natural Science Foundation of China under Grant U19B2029, Grant 61803222, and Grant 61873140; and in part by the Independent Research Program of Tsinghua University under Grant 2018Z05JDX002. The Associate Editor coordinating the review process was Yan Zhuang. *(Corresponding author: Ziyang Meng.)*

The authors are with the Department of Precision Instrument, Tsinghua University, Beijing 100084, China (e-mail: wangjunrob@mail.tsinghua.edu.cn; ziyangmeng@mail.tsinghua.edu.cn; wlei16@mail.tsinghua.edu.cn).

Digital Object Identifier 10.1109/TIM.2021.3072130

The main contributions of this article are as follows.

1) A region-based particle filter is proposed to initialize the locations of the landmarks. A proper likelihood model is designed to adapt to this approach such that efficient processing is realized. Moreover, the proposed approach also allows the measurements of new landmarks to act on the self-localization of the mobile robot without delayed processing.
2) A coarse detection method is used to eliminate the effect of the outliers when using a nonparametric approach to estimate the landmark location. The coexistence of loose coupling and tight coupling can reduce the computation burden and improve the adaptability to the outliers.
3) The proposed RO-SLAM algorithm is applied to a UWB-based localization system. The superiority of the proposed method compared with conventional Rao-Blackwellized particle filters (RBPF)-based RO-SLAM is explained in a simulation environment. Moreover, the validity of the proposed RO-SLAM algorithm is also verified in the real environment.

This article is organized as follows. The classical RO-SLAM schemes are discussed in Section II. In Section III, the proposed RO-SLAM algorithm is introduced in detail. The validity and superiority of the proposed algorithm are demonstrated using the simulations and experiments in Section IV and Section V, respectively. The conclusions are drawn in Section VI.

II. Related Works

Classical algorithms in the RO-SLAM utilize the EKF [9], RBPF [7], Sparse Extended Information Filter (SEIF) [10], and graph optimization methods [11]. Optimization techniques are employed to RO-SLAM with smoothing and mapping (SAM) in [11] and GraphSLAM in [12] after the initialization of the landmarks is finished. In [13], a spectral learning approach is presented. Blanco *et al.* [5] proposed the utilization of particle filter to initialize the landmark locations based on the FastSLAM framework. The EKFs used for updating the landmark locations in each particle are replaced by particle filters in the initialization stage to avoid the need for bearing measurements. Shue *et al.* [6] use the adaptive character of the particle filter to make the multipath interference less impactful to the overall state estimation of RO-SLAM. Kim and Kim [7] extended to use the particle filter for the initialization of the nodes in cooperative RO-SLAM. The particle filter is capable of handling the non-Gaussian distribution inherited in the RO-SLAM problem and the particles can rapidly converge into Gaussian distribution within a few iterations. According to these characters, the particle filter is adapted to initialize the landmark location in this article. From the initialization perspective, the RO-SLAM algorithms can be also classified into delayed and undelayed ones.

In the delayed methods, the position of the landmark is inserted into the filter until enough measurement information is available to localize this landmark. Leonard *et al.* [14] initialized different kinds of features from range measurements by incorporating the associated robot poses. Sufficient measurements could improve the accuracy of the initialization of the landmark while the long delay could lead to the accumulated odometry errors that affect the initialization of the landmark. Olson *et al.* [15] utilized a voting scheme over a 2-D probabilistic grid to achieve an initial estimation of each landmark. The landmark position is initialized using the cell in the grid with a higher ratio of votes. Zhou [16] utilized the trilateration method to realize the delayed initialization of the landmarks. Although it is very simple, this approach is very sensitive to outliers. Another solution [5] is to use a particle filter to initialize the landmark locations based on the FastSLAM framework. In the beginning, the probability density is uniformly distributed around a circle centered on the position of the robot. The radius of this circle is the first range measurement. The weight of each particle is updated according to the following range measurements. The mean and variance will be used to initialize the landmark when these particles converge to a single location.

For the undelayed methods, the hypotheses of the location of the landmark with non-Gaussian distribution are applied to the filter. The state of the landmark is commonly represented by a multimodal distribution. The bad hypotheses can be pruned according to the newly available measurements until a single hypothesis remains. Caballero *et al*. [17] and Fabresse *et al*. [18] use the mixture of Gaussians to initialize the position of the landmark. Each hypothesis is linked with a weight which is updated according to the likelihood that a range measurement satisfies this hypothesis. When a weight falls below a threshold, the corresponding hypothesis is removed from the filter. This method provides good performances but at a high computational cost, positively related to the number of hypotheses. Djugash and Singh [19] use relative-over parametrized (ROP) EKF for the RO-SLAM problem. The pose of the robot and the positions of landmarks are expressed in polar coordinates. This method is more robust than the standard Euclidean formulation in the case of poor initialization, sparse data, and incorrect data association due to its improved representation of the state uncertainty.

The main advantage of the underlying approach is that the information provided by the range measurements can be used to update the filter for modifying the estimation of the robot pose from the very beginning. However, the initialization using particle filter is difficult to achieve an undelayed performance which makes the robot localization can benefit from the measurements as soon as possible. In particular, a large number of particles are needed to spread all possible positions and to avoid the influence of the outliers generated from the range-only sensors in the early stages to ensure accuracy. However, this approach increases the computation burden seriously. Therefore, it is desirable to achieve low computation cost and undelayed performance using the particle filter. We next detail an algorithm addressing these issues.

III. Problem Formulation and Proposed Algorithm

A. Problem Formulation

Using a probabilistic approach to RO-SLAM is to achieve the joint probability distribution of the robot pose (or path)

and the map. Motivated by the strong non-Gaussian distributions found in RO-SLAM, we propose to address the RO-SLAM problem in a 2-D scene by maximizing the following probability:

$$p(\boldsymbol{x}_t, \boldsymbol{m_t} \mid z_t, \boldsymbol{u}_t) = p(\boldsymbol{x}_t \mid z_t, \boldsymbol{u}_t) p(\boldsymbol{m_t} \mid \boldsymbol{x}_t, z_t, \boldsymbol{u}_t) \quad (1)$$

where $\boldsymbol{x}_t = (x_t, y_t, \theta_t)^T$ and $\boldsymbol{m_t}$ denote the pose of the mobile robot and the map at time t, respectively. In addition, $\boldsymbol{u}_t$ denotes the control variable and z_t means the observation.

RBPF stores a conditional distribution of the map for each robot path hypothesis and assumes the errors in the measurements are mutually independent. Therefore, (1) can be further factorized in the following form:

$$p(\boldsymbol{x}_t, \boldsymbol{m_t} \mid z_t, \boldsymbol{u}_t) = p(\boldsymbol{x}_t \mid z_t, \boldsymbol{u}_t) \prod_{n=1}^{N} p\left(\boldsymbol{m}_{n,t} \mid \boldsymbol{x}_t, z_t, \boldsymbol{u}_t\right) \quad (2)$$

where $\boldsymbol{m}_{n,t} = (x_{n,t}, y_{n,t})^T$ denotes the detected landmark at time t and N is the number of landmarks. The FastSLAM algorithm proposed by Montemerlo *et al.* [20], is an effective RBPF-based SLAM algorithm. The location of each landmark is represented by the mean and covariance of the Gaussian distribution and updated by the EKF algorithm. According to the non-Gaussian distribution of RO-SLAM, for each landmark that is observed for the first time, an independent particle filter is generated to perform the Bayesian estimation of the new landmark. Then, this particle filter eventually converges from the initial circular shape toward a small Gaussian-like shape, and it will be replaced (without loss of the estimated uncertainty) by a standard EKF which performs reliably for reduced uncertainties.

However, the conventional particle filter needs a large number of particles to approximate the landmark posterior. Moreover, measurements obtained from the landmark before the initialization is difficult to be used in the filter for the estimation of robot localization. To solve these problems, we propose a region-based particle filter and a novel likelihood model for the initialization of the landmark in the RO-SLAM.

B. Algorithm

We use a loosely coupled approach to the location estimation of the landmarks that have not converged into a Gaussian-like shape and the pose estimation of the robot. The pose of the robot is estimated using a robot particle set of $\boldsymbol{Y}_{r,t} = \left(\boldsymbol{y}_t^1, \ldots, \boldsymbol{y}_t^I\right)$. I is the number of robot particles. When no landmark achieves the Gaussian distribution, the state vector of each robot particle $\boldsymbol{y}_t^i$ is of the following form:

$$\boldsymbol{y}_t^i = < \boldsymbol{x}_t^i, \omega_t^i > \quad (3)$$

where $\boldsymbol{x}_t^i = \left(x_t^i, y_t^i, \theta_t^i\right)^T$ denotes the state of robot particle i, and ω_t^i is importance weight. Each landmark location is estimated by using an independent region-based landmark particle set of $\boldsymbol{Y}_{n,t} = \left(\boldsymbol{y}_{n,t}^{[1]}, \ldots, \boldsymbol{y}_{n,t}^{[C]}\right)$ before converging into a Gaussian distribution. C is the number of landmark particles used to initialize landmark n. The parameters of the landmark particles are not included in the state vector of the robot particle. The landmark particle is of the form

$$\boldsymbol{y}_{n,t}^{[c]} = < \boldsymbol{m}_{n,t}^{[c]}, \beta_{n,t}^{[c]}, S\theta_{n,t}^{[c]}, L\theta_{n,t}^{[c]}, r_n^{[c]}, \boldsymbol{x}_{n,t_0} > \quad (4)$$

where $\boldsymbol{m}_{n,t}^{[c]} = \left(x_{n,t}^{[c]}, y_{n,t}^{[c]}\right)^T$ denotes the location of landmark particle c for initializing landmark n at time t ($1 \le c \le C$ and $1 \le n \le N$). $S\theta_{n,t}^{[c]}$ and $L\theta_{n,t}^{[c]}$, respectively, denote the minimum and maximum radians of the region represented by particle c. $r_n^{[c]}$ and $\boldsymbol{x}_{n,t_0} = (x_{n,t_0}, y_{n,t_0})^T$ denote the range measurement and position of the robot when landmark n is first detected, respectively. In addition, $\beta_{n,t}^{[c]}$ denotes the weight of landmark particle c.

When the particles of a landmark converge to a Gaussian distribution, a tightly coupled approach is used to estimate this landmark location and robot pose. The particles for estimating this landmark are deleted and the Gaussian parameters for updating this landmark are inserted into the robot particles. The state vector for the particle $\boldsymbol{y}_t^i$ that all the landmarks have converged to Gaussian distribution is of the following form:

$$\boldsymbol{y}_t^i = < \boldsymbol{x}_t^i, \omega_t^i, \boldsymbol{\mu}_{1,t}^i, \boldsymbol{\xi}_{1,t}^i, \ldots, \boldsymbol{\mu}_{N,t}^i, \boldsymbol{\xi}_{N,t}^i > \quad (5)$$

where $\boldsymbol{\mu}_{n,t}^i = (x_{n,t}^i, y_{n,t}^i)^T$ and $\boldsymbol{\xi}_{n,t}^i$ indicate the mean vector and covariance matrix of the Gaussian distribution which is used to represent the location of the landmark n. During the movement of the mobile robot, the loosely coupled and tightly coupled forms may coexist in the SLAM process according to the status of the landmarks.

1) Prediction Step: The position and orientation of the mobile robot in each particle are first updated by the motion model and can be expressed as

$$\boldsymbol{x}_t = \boldsymbol{f}(\boldsymbol{x}_{t-1}, \boldsymbol{u}_t) + \boldsymbol{\delta}_t \quad (6)$$

where $\boldsymbol{x}_t$ denotes the pose of the mobile robot at time t and $\boldsymbol{u}_t$ denotes the control variable. In addition, $\boldsymbol{\delta}_t$ is the motion noise, and is assumed to follow a zero-mean Gaussian distribution with covariance $\boldsymbol{Q}_t$. Then, the update step will be executed according to the landmark status.

2) Update Step With Non-Gaussian Distribution: When a landmark is first observed, a particle filter is used to initialize the location of this landmark. Conventional approaches use particles to represent the potential locations where the landmark is. These particles are distributed around a circle centered on the robot's position where the robot first detects the landmark. The radius of this circle is the range measurement. To ensure the localization accuracy, Blanco et al. [5] used a heuristic rule $N = \alpha \cdot r_n$ to set the number N of the particles, where α can vary from 400 to 2000 and r_n is the range measurement when landmark n is first detected. Although Blanco *et al.* [5] reduced the computational burden by dropping particles according to the weights, the number of the particles is also quite large in the early stage.

In this article, we propose to use each particle to represent one region of the uniform distribution of the landmark. When landmark n is first detected, a set of landmark particles are assigned to estimate its location. Because the distribution of the landmark in the first detection is a ring shape, the particles divide this circle through angles as shown in Fig. 1. Each landmark particle represents an arc that potentially contains the true landmark location. The parameters to represent this arc are stored in (4). The weights of these landmark particles are set to be 1.

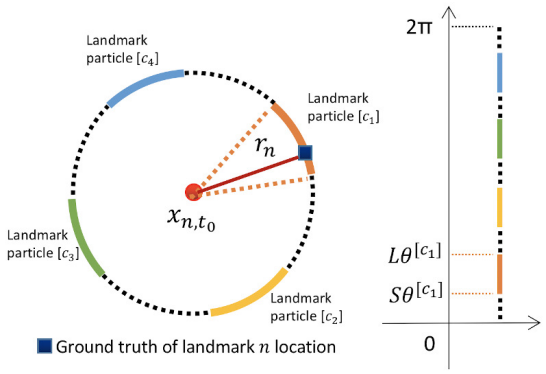

Fig. 1. Initialization of region-based landmark particles (the omitted particles are represented by dots).

An illustration of the update process for the landmark particles and robot particles with the following detection for landmark n is shown in Fig. 2. First, the weights of the landmark particles are updated using the likelihood function to reduce the uncertainty and make the particles converge into a Gaussian distribution. To cope with the region-based particle, a proper likelihood function is proposed in this article. The likelihood function of the landmark particle is designed based on the idea that if the landmark particle has an accurate estimation, the region represented by this particle will overlap with the ring region built by the current robot location and measurement. The approach to evaluate the overlap is to check whether the current measurement value is included in the shortest and longest distance from the current robot position to the region of the landmark particle. The likelihood function of the landmark particle is expressed by a piecewise function

$$\begin{aligned}\beta_{n,t}^{[c]} &= \boldsymbol{g}\left(\boldsymbol{x}_t, \boldsymbol{y}_{n,t}^{[c]}\right) \\ &= \begin{cases} 1, & \text{if } Sr_{n,t}^{[c]} < r_t < Lr_{n,t}^{[c]} \\ \bar{\boldsymbol{g}}\left(\min\left(|r_t - Sr_{n,t}^{[c]}|, |r_t - Lr_{n,t}^{[c]}|\right)\right), & \text{else} \end{cases}\end{aligned} \tag{7}$$

where r_t is the current range measurement. In addition, $Sr_{n,t}^{[c]}$ and $Lr_{n,t}^{[c]}$ are the shortest distance and longest distance between the robot position $\boldsymbol{x}_t$ and the arc represented by particle c as shown in Fig. 2(a). if the current measurement value is within the shortest and longest distance from the robot location to the region represented by landmark particle c, the weight of landmark particle c is set to 1. By taking into the noise account, the weight of the landmark particle that does not satisfy this condition is not set to be 0. Instead, the difference between the current measurement with the shortest and longest distances are, respectively, calculated. The smaller difference is the shortest distance between the region represented by the landmark particle and the ring region built by the current robot location and measurement. The weight of this kind of landmark particle is defined by substituting this smaller difference into the exponential function $\bar{\boldsymbol{g}}$. In addition, $Sr_{n,t}^{[c]}$ and $Lr_{n,t}^{[c]}$ are obtained using

$$Sr_{n,t}^{[c]} = \begin{cases} |r_n^{[c]} - d_{n,t}^{[c]}|, & \text{if } S\theta_{n,t}^{[c]} < \theta_{n,t}^{[c]} < L\theta_{n,t}^{[c]} \\ \min\left(Sd_{n,t}^{[c]}, Ld_{n,t}^{[c]}\right), & \text{else} \end{cases} \tag{8}$$

$$Lr_{n,t}^{[c]} = \max\left(Sd_{n,t}^{[c]}, Ld_{n,t}^{[c]}\right), \tag{9}$$

where $d_{n,t}^{[c]} = |\boldsymbol{x}_t - \boldsymbol{x}_{n,t_0}|$, $\theta_{n,t}^{[c]} = \arctan(y_t - y_{n,t_0}, x_t - x_{n,t_0})$, $Sd_{n,t}^{[c]} = \left|\boldsymbol{x}_t - \boldsymbol{Sx}_{n,t}^{[c]}\right|$, and $Ld_{n,t}^{[c]} = \left|\boldsymbol{x}_t - \boldsymbol{Lx}_{n,t}^{[c]}\right|$. $\boldsymbol{Sx}_{n,t}^{[c]}$, and $\boldsymbol{Lx}_{n,t}^{[c]}$ are the coordinates of the two ends of the arc represented by particle c, and calculated using

$$\begin{aligned}\boldsymbol{Sx}_{n,t}^{[c]} &= \boldsymbol{x}_{n,t_0} + r_n^{[c]} \cdot \begin{pmatrix} \cos\left(S\theta_{n,t}^{[c]}\right) \\ \sin\left(S\theta_{n,t}^{[c]}\right) \end{pmatrix} \\ \boldsymbol{Lx}_{n,t}^{[c]} &= \boldsymbol{x}_{n,t_0} + r_n^{[c]} \cdot \begin{pmatrix} \cos\left(L\theta_{n,t}^{[c]}\right) \\ \sin\left(L\theta_{n,t}^{[c]}\right) \end{pmatrix}. \end{aligned} \tag{10}$$

The exponential function $\bar{\boldsymbol{g}}$ is defined as

$$\bar{\boldsymbol{g}}(d_t) = \exp\left(-\frac{d_t^T d_t}{2\sigma_z^2}\right) \tag{11}$$

where σ_z denotes the covariance of the observation Gaussian noise.

Then, the resampling step is introduced based on the weights of landmark particles. When the weight of a landmark particle is less than 0.01, this particle is reassigned to represent the half arc region of the landmark particle with a large weight. The landmark particle with the large weight is also reassigned to represent the other half arc region. Fig. 2(b) shows the process of resampling step that particles c_2 and c_3 with the small weights are, respectively, reassigned to represent the half arc region of landmark particles c_1 and c_4. Particles c_1 and c_4 are reassigned to represent the other half arc region. Thus, the uncertainty is gradually deleted and the landmark particles gradually converge to a small region based on the following measurements. The location of landmark n is updated based on the resampled landmark particles

$$\boldsymbol{m}_{n,t} = \sum_{c=1}^{C} \beta_{n,t}^{[c]} \boldsymbol{m}_{n,t}^{[c]} / \sum_{c=1}^{C} \beta_{n,t}^{[c]}. \tag{12}$$

The weights of robot particles can be updated based on the detected landmark without delay processing. The likelihood function of the robot particle is also designed based on the idea that if the robot particle has an accurate estimation, the ring region built by the location of this robot particle and current measurement will overlap the landmark potential region. The potential region of the landmark is the area covered by all resampled landmark particles as shown in Fig. 2(c). The approach to evaluate the overlap is to check whether the current measurement value r_t is included in the shortest and longest distance from the robot particle position to the potential region of the detected landmark. The weight of robot

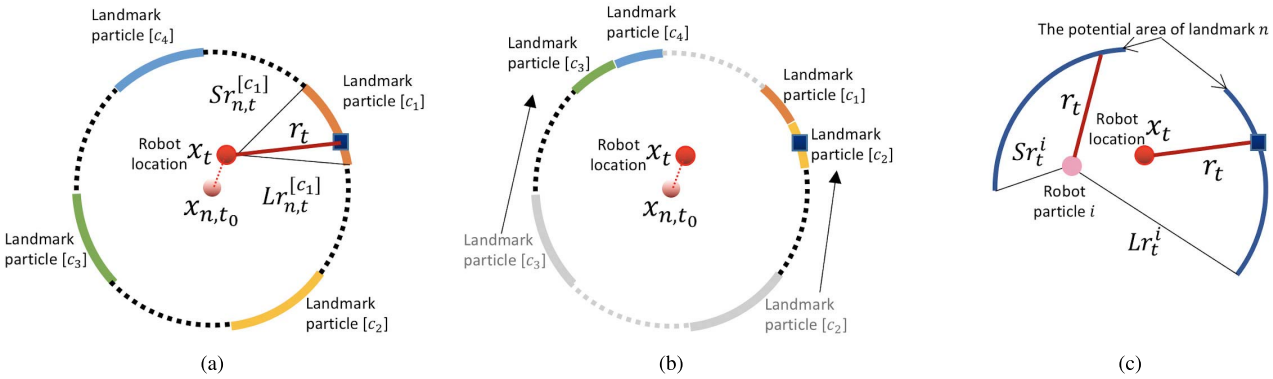

Fig. 2. Update of landmark particles and robot particles if it is not the first detection for the current detected landmark. (a) Calculation of landmark particle weights. (b) Resampling of landmark particles (the gray part is the region of the eliminated particles). (c) Calculation of robot particle weights.

particle i is calculated by using the likelihood function as

$$\omega_t^i = \boldsymbol{g}(\boldsymbol{x}_t^i, \boldsymbol{Y}_{n,t}) = \begin{cases} 1, & \text{if } Sr_t^i < r_t < Lr_t^i \\ \bar{\boldsymbol{g}}\left(\min\left(|r_t - Sr_t^i|, |r_t - Lr_t^i|\right)\right), & \text{else} \end{cases} \tag{13}$$

where Sr_t^i and Lr_t^i are the shortest distance and the longest distance between the location of robot particle i and the potential region of landmark n. Sr_t^i and Lr_t^i can be achieved by referring to the calculation method of $Sr_{n,t}^{[c]}$ and $Lr_{n,t}^{[c]}$. Lastly, the pose of the mobile robot is updated after the resampling step by using the weights and states of the robot particles

$$\boldsymbol{x}_t = \sum_{i=1}^{I} \omega_t^i \boldsymbol{x}_t^i \Big/ \sum_{i=1}^{I} \omega_t^i. \tag{14}$$

When the uncertainty of the landmark estimation is eliminated so that it can be represented by a Gaussian distribution, the location of the landmark is estimated by EKF. In our implementation, we check whether a given distribution of a landmark should be transformed to a Gaussian by obtaining the arc length between the largest and smallest radian of this landmark's potential area and then check whether this arc length is below a given threshold.

3) Update Step With Gaussian Distribution: It is a tightly coupled form between the estimation of the landmark with a Gaussian distribution and the estimation of the robot. The mean vector and covariance matrix of the landmark are inserted in the state vector of each robot particle. To transform the distribution of a landmark to the Gaussian from the particle filter, the range $r_{n,t}$ and bearing $\theta_{n,t}$ between the robot and landmark are obtained by using a nonlinear function $\bar{\boldsymbol{h}}$

$$r_{n,t} = \sqrt{\left(x_t - x_{n,t}\right)^2 + \left(y_t - y_{n,t}\right)^2} \tag{15}$$

$$\theta_{n,t} = \arctan \frac{y_t - y_{n,t}}{x_t - x_{n,t}}. \tag{16}$$

The mean $\boldsymbol{\mu}_{n,t}$ of the landmark location in each robot particle is initialized by using

$$\boldsymbol{\mu}_{1,t}^i = \boldsymbol{x}_t^i + \begin{pmatrix} r_{n,t}\cos\left(\theta_{n,t}\right) \\ r_{n,t}\sin\left(\theta_{n,t}\right) \end{pmatrix}. \tag{17}$$

The covariance matrix is proportional to the arc length between the largest and the smallest radian of the landmark's potential area.

Then, the estimation of the landmark in each particle i is realized via a standard EKF

$$\boldsymbol{S}_t = \boldsymbol{H}_t \boldsymbol{\xi}_{n,t}^i \boldsymbol{H}_t^T + \sigma_z \tag{18}$$

$$\boldsymbol{K}_t = \boldsymbol{\xi}_{n,t}^i \boldsymbol{H}_t^T \boldsymbol{S}_t^{-1} \tag{19}$$

$$\boldsymbol{\mu}_{n,t}^i = \boldsymbol{\mu}_{n,t-1}^i + \boldsymbol{K}_t\left(r_t - d_{n,t|t-1}^i\right) \tag{20}$$

$$\boldsymbol{\xi}_{n,t}^i = (I - \boldsymbol{K}_t \boldsymbol{H}_t)\boldsymbol{\xi}_{n,t-1}^i \tag{21}$$

where $d_{n,t|t-1}^i$ denotes the distance between the current robot location and the landmark location at time $t-1$ in robot particle i

$$d_{n,t|t-1}^i = \sqrt{\left(x_t^i - x_{n,t|t-1}^i\right)^2 + \left(y_t^i - y_{n,t|t-1}^i\right)^2}. \tag{22}$$

In addition, $\boldsymbol{H}_t$ is the Jacobian matrix [3], [21] of function in (22) with respect to the landmark coordinate

$$\boldsymbol{H}_t = \left(\frac{\left(x_{n,t}^i - x_t^i\right)}{d_{n,t|t-1}^i}, \frac{\left(y_{n,t}^i - y_t^i\right)}{d_{n,t|t-1}^i} \right). \tag{23}$$

The weight of each particle is calculated using the updated landmark location by the exponential function $\hat{\boldsymbol{g}}$

$$\omega_t^i = \omega_{t-1}^i \hat{\boldsymbol{g}}\left(r_t, d_{n,t}^i\right) \tag{24}$$

where $d_{n,t}^i$ denotes the distance between the current robot location and the updated landmark location in particle i. Finally, the states of the robot and landmark are updated using (14) after the resampling step.

C. Removal of Ranging Outliers

Outliers occur regularly due to multipath effects and/or non-line-of-sight (NLOS) conditions. The outliers are crucial to the accuracy of the RO-SLAM problem since nonnegligible positive biases are introduced in the range measurements [22], [23]. A hypothesis testing on the residuals/innovations $\bar{z}^i = r_t - d_{n,t|t-1}^i$ of EKF is used to distinguish the outliers in [24]. Except for outliers, the residuals should satisfy

$$\bar{z}^i \sim \mathcal{N}(0, \boldsymbol{S}_t). \tag{25}$$

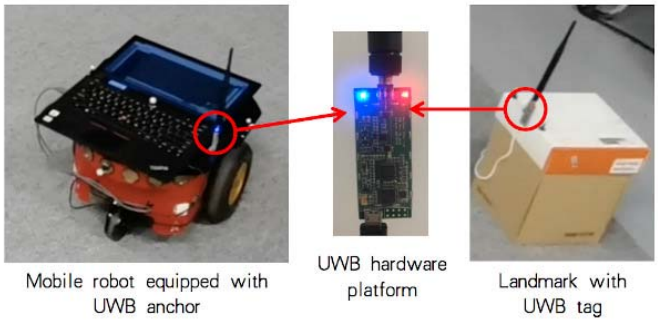

Fig. 3. UWB-based localization system utilized in this article.

If a range measurement is out of the given confidence interval, this range is considered as an outlier and is ignored. This method is a very common way to remove outliers and is used in the proposed algorithm when the distribution of the detected landmark is a Gaussian distribution.

However, this approach cannot distinguish the outliers when the landmark is estimated by the nonparametric particle filter. In particular, the outlier occurs when the detected landmark with non-Gaussian distribution has greater impacts on the accuracy of the landmark estimation. The outliers are likely to cause the landmark particles to converge far from the true landmark location. Therefore, we use a coarse method to remove outliers for the range measurement obtained from the landmark estimated by the particle filter. Motivated by the idea of [25], the criterion is extended as

$$\begin{cases} 0, & \text{if } \Delta \boldsymbol{x}_{k|k-1} > \zeta \text{ or } k = 1 \\ 1, & \text{else if } r_{n,k} \le r_{n,k-1} + \Delta \boldsymbol{x}_{k|k-1} + W_z \\ -1, & \text{else} \end{cases} \tag{26}$$

where 0, 1, and -1 are, respectively, indicates the actions of temporary storage, utilization and removal. $r_{n,k}$ is the range measurement obtained from landmark n and k means the index of the detection times, $\Delta \boldsymbol{x}_{k|k-1}$ is the moving distance of the mobile robot during the detection from $k-1$ to k, and ζ is a threshold to avoid the $\Delta \boldsymbol{x}_{k|k-1}$ is too large to restrict the outliers. ζ is set based on the speed of the mobile robot and the sampling frequency of the sensor. In addition, W_z denotes the accuracy of the sensor. For the situation that $r_{n,k}$ belongs to condition 1 of (26) and the relationship between $r_{n,k}$ and $r_{n,k+1}$ does not satisfy condition 2 of (26), $r_{n,k+2}$ is used to judge the outlier in $r_{n,k}$ and $r_{n,k+1}$.

IV. Applications to UWB-Based Localization System

The proposed algorithm is applied to an UWB-based localization system. UWB MINI3S PLUS is adopted in the system as shown in Fig. 3. Four UWB tag devices are placed on the floor as static landmarks. One anchor is installed on the mobile robot. We utilize a predefined value to realize the calibration of spatial position between the anchor and the tracked point of the mobile robot. This anchor actively requests the distance to the landmarks in a timely fashion. The motion model of the nonholonomic mobile robot [26] of Pioneer 3-DX is defined as

$$\begin{aligned} \boldsymbol{x}_t &= \boldsymbol{f}(\boldsymbol{x}_{t-1}, \bar{v}_{t-1}, \bar{\omega}_{t-1}) + \boldsymbol{\delta}_t \\ &= \begin{pmatrix} x_{t-1} \\ y_{t-1} \\ \theta_{t-1} \end{pmatrix} + \begin{pmatrix} \bar{v}_{t-1}\cos\theta_{t-1} - d \cdot \bar{\omega}_{t-1}\sin\theta_{t-1} \\ \bar{v}_{t-1}\sin\theta_{t-1} + d \cdot \bar{\omega}_{t-1}\cos\theta_{t-1} \\ \bar{\omega}_{t-1} \end{pmatrix} \Delta T \\ &\quad + \boldsymbol{\delta}_t \end{aligned} \tag{27}$$

where $\boldsymbol{x}_t = (x_t, y_t, \theta_t)^T$ denotes the position and orientation of the mobile robot, $\bar{v}_{t-1}$ is the forward velocity and $\bar{\omega}_{t-1}$ is the angular velocity of the mobile robot. In addition, d is the distance in the forward direction of the mobile robot from the rear axis center to the point being tracked, and ΔT is the sampling time.

The system error of UWB hardware is also considered. To modify the influence of the system error, we use the experimental method to obtain the relationship between the measurement value and the groundtruth. The experiment scene is shown in Fig. 4(a). The UWB anchor and the tag are set to the same height. The tag moves away from the anchor and the measurements are recorded at every 10 cm movement. When the moving distance exceeds 500 cm, the tag moves 20 cm each time. The average values of the measurements at each recorded point are shown in Fig. 4(b). Then, we use the least-squares method to fit these data and obtain the fitting function

$$\bar{r}_t = 0.99 r_t - 7.94 \tag{28}$$

where $\bar{r}_t$ is the modified measurement. In this way, the system errors of the UWB system used in this article can be effectively eliminated.

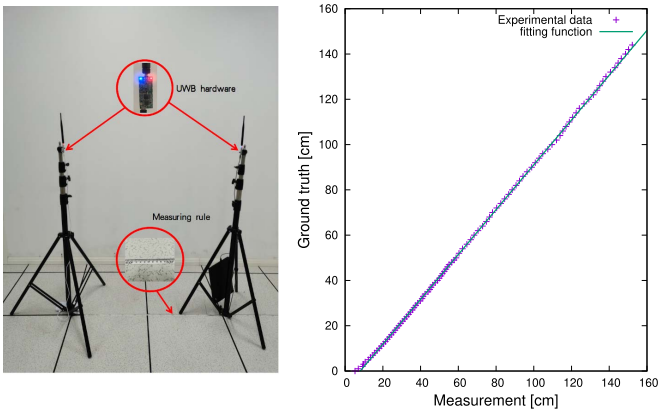

(a) (b)

Fig. 4. (a) Set up of the experiment to test the system errors. (b) Measurements and fitting function.

V. Simulation Verifications

The proposed RO-SLAM algorithm is evaluated in simulations using the UWB detection model. A maximum detection range of 20 m has been considered in the simulated sensor to allow the mobile robot to discover new landmarks as it moves. Measurements are also corrupted by Gaussian noise with $\sigma_r = 0.05$ m. Using the same experimental setup, we also compare the proposed algorithm with the RO-SLAM algorithm of Blanco *et al.* [5] that uses the conventional point-based

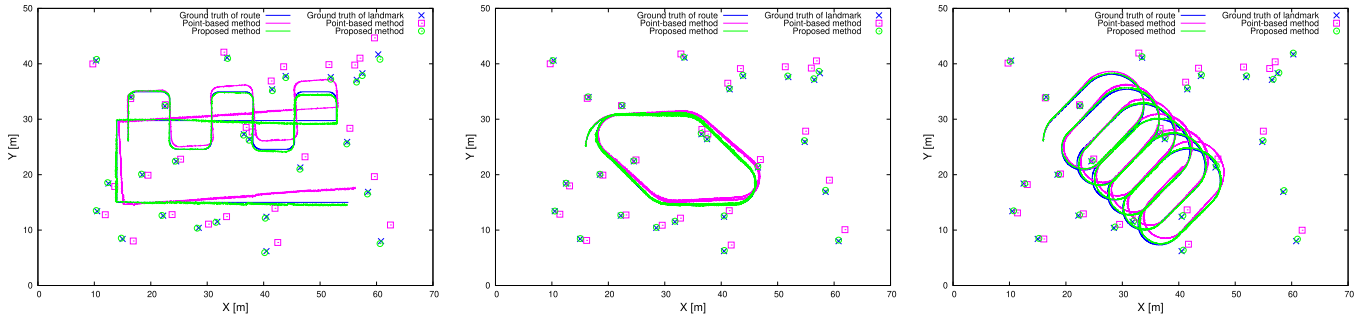

Fig. 5. Performances of the proposed algorithm and algorithm [5] at three different trajectories.

TABLE I

ERRORS OF THE ROBOT PATH AND LANDMARK LOCATIONS ESTIMATED BY USING THE PROPOSED METHOD AND THE POINT-BASED METHOD IN SIMULATION

Method	Trajectory 1			Trajectory 2			Trajectory 3		
	Robot pose		Tag location	Robot pose		Tag location	Robot pose		Tag location
	d_r [m]	θ [rad]	d_t [m]	d_r [m]	θ [rad]	d_t [m]	d_r [m]	θ [rad]	d_t [m]
Point-based method	1.025	0.049	1.235	1.254	0.062	1.798	0.856	0.050	2.261
Proposed method	0.282	0.015	0.247	0.267	0.020	0.301	0.157	0.013	0.152

particle filter to realize the initialization of the landmark. The number of the landmark particles used in the point-based method is set according to the heuristic rule $N = \alpha \cdot r_n$ given in [5], α is set to be 400 in this section. The number of robot particles is set to be 100. Our proposed method uses 40 landmark particles to estimate the landmark with the non-Gaussian distribution and 100 robot particles to estimate the robot pose and the landmark with the Gaussian distribution.

A. Accuracy

Three trajectories are simulated in the environment to verify the accuracy of the two algorithms. The simulated environment with a size of 40 $\times$ 60 m is set with 26 landmarks. The outlier interference of the range measurement is added in the simulations.

Fig. 5 shows the performances of the robot path and landmark locations using the proposed algorithm and the point-based method. The routes of the robot and landmark locations estimated by the proposed method present better coincidence with the groundtruth than those of the point-based method. In particular, Fig. 5(c) shows that the outliers lead to two landmarks estimated by using the point-based method out of the simulated environment. The outlier occurs when the detected landmark with non-Gaussian distribution easily causes the landmark particles converging to a wrong estimation. The box plot of the landmark localization errors generated by using the proposed method and the point-based method is shown in Fig. 6. According to the obtained results, the errors generated by using the point-based method are larger than those of the proposed method on three trajectories. Moreover, the distribution of the 26 landmark location errors generated by using the point-based method is dispersed. In particular, two large outliers appear on trajectory 3 by using the point-based method. In contrast, our proposed algorithm achieves more consistent results.

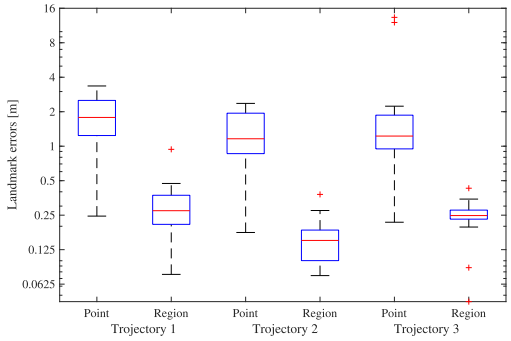

Fig. 6. Box plot of the landmark localization errors generated by using the proposed method and the point-based method.

The errors of the robot and landmark localization produced by two RO-SLAM algorithms on three trajectories are listed in Table I. The errors are computed as the Euclidean distance between the estimated and groundtruth values. The error of the robot path listed in the tables is the mean of the errors for the complete path. The error of the landmark location list in the tables is the mean of the distance deviation between the final estimated locations and groundtruth values of all detected landmarks. According to these data, the proposed method obtains better accuracy for both the robot and landmark localization on three trajectories. The large errors of the point-based SLAM algorithm are generated because the size of the simulated environment is relatively large so that the accumulated errors are increasingly generated. The point-based SLAM algorithm cannot effectively eliminate this accumulated error. Moreover, the accumulated errors also affect the estimation of the landmarks. The undelayed processing of the proposed algorithm allows the mobile robot to achieve the most recent observations from the new landmarks and improve the accuracy of the self-localization. The region-based particle

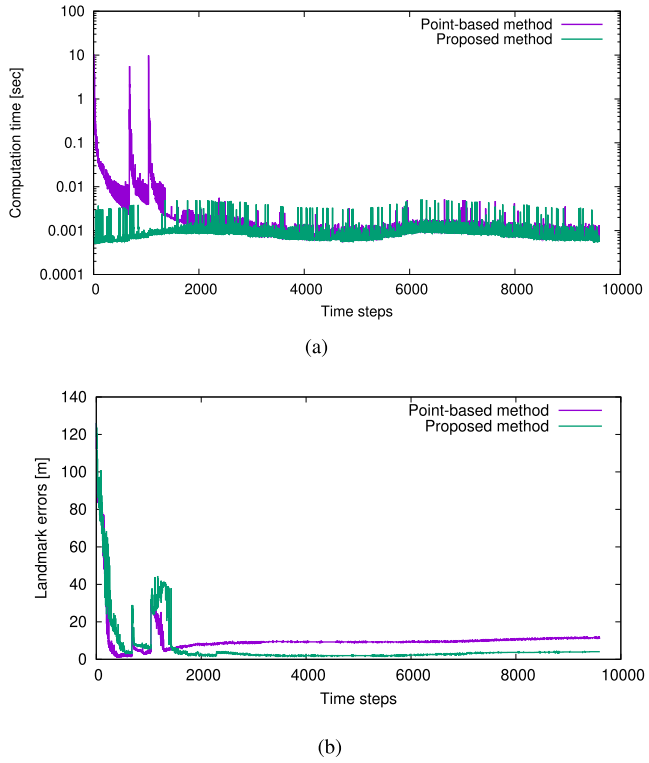

Fig. 7. (a) Computation time at each time step. (b) Errors of the landmarks at each time step.

filer and outlier removal method effectively mitigate the influence of the measurements with large errors for the landmark localization.

B. Efficiency

We next test the proposed method in a simulated environment to demonstrate the efficiency of the proposed algorithm. Twelve landmarks are placed in the simulation and the robot is set to run a circular path. Ten landmarks are detected from the beginning, and two landmarks are detected during the movement to demonstrate the ability to incorporate new landmarks at arbitrary instants of time.

Fig. 7(a) shows the computational time required by each iteration of two SLAM algorithms. The computation time of the point-based RO-SLAM algorithm depends on how many landmarks are observed and their representation in the RBPF particles. In particular, for the particle-based representation, the time consumed is proportional to the number of particles, while for the Gaussian representation a fixed time is required to update the EKF. The proposed method is not affected by these two aspects. A loosely coupled approach increases the scalability to deal with a large number of landmarks without consuming a lot of computational time. The region-based particle filter only needs a few particles to estimate the location of the landmark. Therefore, the proposed algorithm needs much less computational time than the point-based method does. Therefore, the proposed method improves computation efficiency and can be used in real-time.

Fig. 7(b) shows the total errors of the detected landmarks in each iteration of two SLAM methods. The point-based

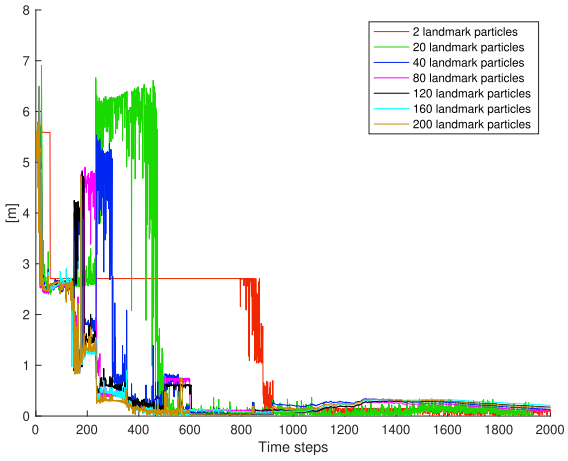

Fig. 8. Performances of the landmark localization with different number of landmark particles.

RO-SLAM algorithm utilizes a large number of particles to fit the locations of the landmarks. The wrong estimation of these particles can be rapidly deleted based on the measurements. However, the result is easily affected by outliers. The region-based particle filter and the coarse detection method for range outliers make the proposed algorithm achieve almost the same iterations as the point-based method does and better accuracy.

C. Performance With Different Number of Landmark particles

The respective performance with the different number of landmark particles is also evaluated. The robot is set to run a circular path to estimate its pose and the landmark location, simultaneously. Seven different numbers of landmark particles are evaluated here.

Fig. 8 shows the setup of the landmark particle number and the error of the landmark localization in each iteration. According to the obtained results, increasing the number of landmark particles has no significant effect on the accuracy. This is because the traditional point-based particle filter needs a lot of particles to cover the ring form distribution and ensure accuracy. However, the proposed region-based particle filter that even uses a small number of particles can also fit the entire ring form distribution by expanding the represented region of each particle. On the other hand, increasing the number of landmark particles within 80 indeed affects the convergence speed of the particles. However, the convergence rate has no obvious change when the number beyond 80. Therefore, the number of the region-based landmark particles is recommended to set between 40 to 80.

VI. Experiment Verifications

The proposed method and the point-based method are evaluated in real environmental experiments using a real robot and the UWB-based localization system. A heavy computation burden is generated when using the point-based particle filter to initialize the landmark location so that the online evaluation is difficult. Therefore, to compare the proposed algorithm

TABLE II
ERRORS OF THE ROBOT PATH AND LANDMARK LOCATIONS GENERATED ON THREE TRAJECTORIES IN THE OFFICE

Method	Trajectory 1		Trajectory 2		Trajectory 3	
	Robot location d_r [m]	Tag location d_t [m]	Robot location d_r [m]	Tag location d_t [m]	Robot location d_r [m]	Tag location d_t [m]
Point-based method	0.146	0.395	0.139	0.385	0.267	1.223
Proposed method	0.132	0.274	0.114	0.144	0.229	0.247

(a)

(b)

Fig. 9. Office experimental environment. (a) Optitrack[3] motion capture system used to achieve the ground truth. (b) Setup of the UWB landmarks and the mobile robot.

with this conventional method, we have gathered the data sets using a real robot while it moves throughout an office and a long corridor. Four landmarks with the UWB tags are set in the environment. The system errors of the UWB sensors are compensated by using (28) for both algorithms. The speed of the mobile robot is set to be 300 mm/s. The numbers of robot particles and landmark particles used in the two algorithms are the same as the first two parts in the simulation. Furthermore, the improvements of region-based particle filer and the novel likelihood model proposed in this article are also tested by using a public laser data set.

A. Office

In the office, an environment with the size of 5 × 5 m is adopted to evaluate the two RO-SLAM algorithms. Fig. 9 shows a snapshot of the experimental setup. Three data sets are gathered by controlling the mobile robot run three random trajectories in the office environment. The groundtruth of the robot path and landmark locations are tracked by the Optitrack[3] motion capture system as shown in Fig. 9(a).

Fig. 10 shows the results obtained by the proposed method and the point-based method. The corresponding ground truth of each trajectory is also shown. The route of mobile robot and landmark locations estimated by the proposed method coincide nicely with the ground truth in each trajectory. In particular, the landmark location estimated by the proposed algorithm demonstrates better coincidence than the point-based method does. As shown in Fig. 10(c), the location of a landmark by using the point-based method has a large deviation from the ground truth due to the outliers occur in the early stage of the initialization step.

The average errors of the robot and tag localization produced by two SLAM algorithms on three trajectories are listed in Table II. Because the size of the experimental environment in the office is much smaller than the setup in the simulation, the accumulated errors of the robot path are smaller than those in simulation. By comparing the results of two SLAM algorithms, our proposed algorithm achieves better accuracy than that of the point-based method in each trajectory. In particular, the outlier has a great influence on the accuracy of the point-based RO-SLAM algorithm. A large error of the point-based algorithm appears on trajectory 3 is because the outliers occur in the early stage of the landmark initialization step. In addition, the landmark particles converge to an unrecoverable wrong estimation. This result verifies the outlier removal method of the proposed algorithm weakens the effect of the outliers and measurements with large errors.

B. Corridor

In the corridor, an environment with the size of 30 × 2 m is adopted to evaluate the two RO-SLAM algorithms. The experimental environment is shown in Fig. 11(a). The robot starts and stops at the same place and the position deviation is used to evaluate the accuracy of the two algorithms and odometry.

Fig. 11(b) shows the performances of the proposed algorithm, the point-based method and odometry over the entire path. When the movement is finished, the odometry produces a large deviation in the x-axis direction compared with the start place. The position deviations of the proposed algorithm, point-based method, and odometry are 0.189, 0.369, and 0.951 m, respectively. According to the result of the experiment, the accumulated errors of the odometry are effectively reduced by the proposed algorithm. The average errors of the landmark locations estimated by the proposed algorithm and the point-based method are 0.159 and 0.327 m, respectively. Our proposed algorithm obtains better performance than that of the point-based method on both the robot and landmark localization.

C. Public Data Set With Laser Scanner

The improvements of region-based particle filer and the novel likelihood model proposed in this article are evaluated by the public data set with a laser scanner. The improvements

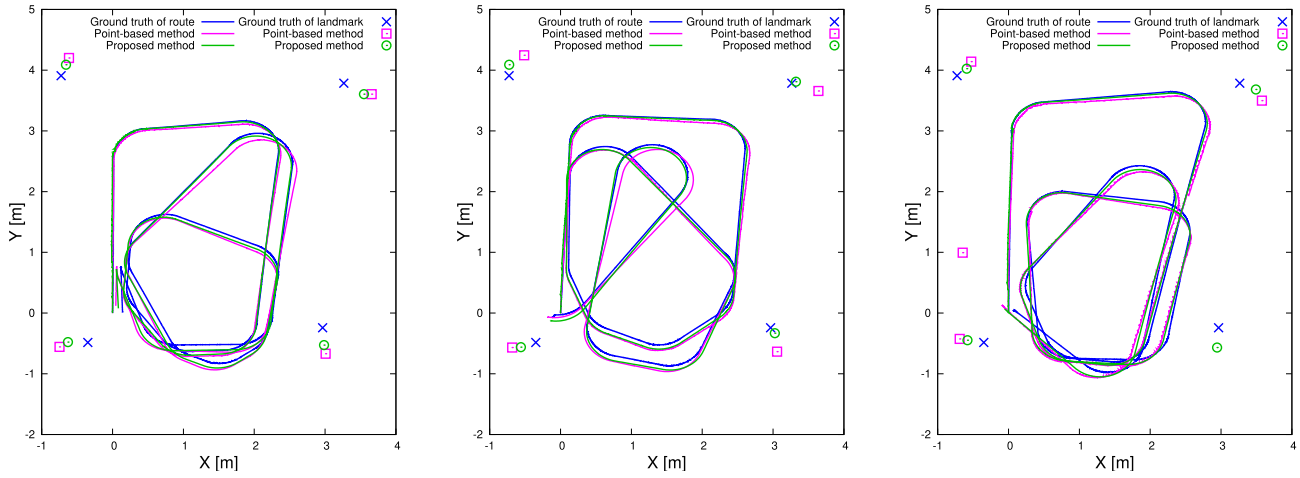

Fig. 10. Results of the proposed method, the point-based method and odometry on three trajectories in the office.

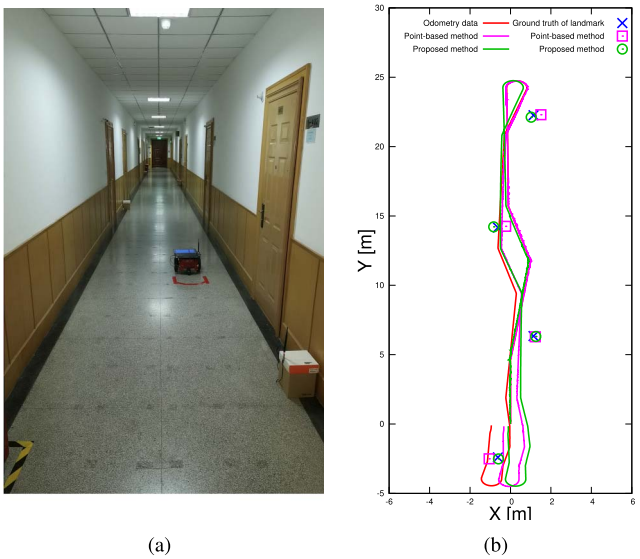

Fig. 11. Corridor experiment. (a) Setup of the UWB landmarks and the mobile robot. (b) Performances of the proposed algorithm, the point-based method, and odometry.

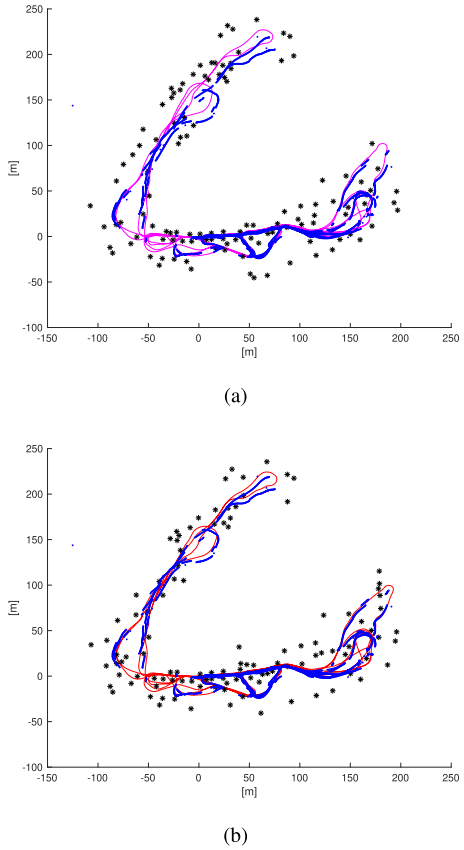

Fig. 12. (a) Results obtained by the point-based method (purple lines). (b) Results obtained by the proposed method (red lines). The blue lines denote the ground truth data from GPS, and the black points are the estimated features.

are used to a SLAM framework [27] that uses particle filters for estimating both the pose of the robot and the location of a landmark. The region-based particle filer is used to replace the point-based particle filter of the original algorithm to estimate the location of the landmark. Each landmark particle represents a sector region that potentially contains the true landmark position. The novel likelihood model is used to update the weights of particles of the robot and landmarks. Then, the improved SLAM algorithm is evaluated using the Sydney Victoria Park data set. The experimental platform was a four-wheeled vehicle equipped with wheel encoders, GPS, and a laser sensor. The GPS data is used as groundtruth data. The improved algorithm and the original algorithm, respectively, use five and one hundred landmark particles for estimating each landmark.

The performance of the improved algorithm is compared with that of the original algorithm. Fig. 12 shows the results obtained by using these two algorithms. According to the results, the paths estimated by the improved algorithm achieve better coincidence with the groundtruth. Moreover, we use GPS data to compare with the estimated paths of the two algorithms. The average errors of the paths estimated by the improved algorithm and original algorithm are 1.28 and 1.66 m, respectively. The average computational costs of the

landmark update required for two algorithms are, respectively, 2.698 and 0.281 ms. According to the results, the improved algorithm obtained better accuracy and efficiency than the original one. Therefore, the improvements of region-based particle filer and the novel likelihood model proposed in this article are also feasible for the laser (Gaussian) detection model.

VII. Conclusion

In this article, a region-based particle filter is proposed based on the RO-SLAM algorithm such that the reduction of particle number is realized and the introduction of new landmarks is allowed without delayed processing. A loosely coupled approach is used to estimate the pose of the mobile robot and locations of the landmarks that have not converged into a Gaussian-like shape. When the particles of a landmark converge to a Gaussian distribution, a tightly coupled approach is used to estimate this landmark location and robot pose. Furthermore, a coarse detection method is proposed to eliminate the effects of outliers on the initialization stage of the landmark. The proposed RO-SLAM algorithm is more robust in the sense of rejecting the outliers and needs less computation cost than conventional approaches. The proposed algorithm is evaluated through simulations and experiments and compared with the conventional RO-SLAM algorithm. The simulated and experimental results verify the validity and superiority of the proposed SLAM algorithm.

Further research includes accelerating the convergence rate of the region-based particles to realize the estimation of the dynamic landmarks [28]. The utilization of the proposed algorithm for the cooperative RO-SLAM [29] and multiple agents [30] will be considered as one of our future directions. Moreover, the fusion of the range-only sensor with the light detection and ranging (LiDAR) [31]–[33] and visual sensors [34]–[36] is also considered as one of our future research.

References

[1] X. Zhu, J. Yi, J. Cheng, and L. He, "Adapted error map based mobile robot UWB indoor positioning," *IEEE Trans. Instrum. Meas.*, vol. 69, no. 9, pp. 6336–6350, Sep. 2020.

[2] V. Magnago *et al.*, "Ranging-free UHF-RFID robot positioning through phase measurements of passive tags," *IEEE Trans. Instrum. Meas.*, vol. 69, no. 5, pp. 2408–2418, May 2020.

[3] L. Geneve, O. Kermorgant, and E. Laroche, "A composite beacon initialization for EKF range-only SLAM," in *Proc. IEEE/RSJ Int. Conf. Intell. Robots Syst. (IROS)*, Sep. 2015, pp. 1342–1348.

[4] E. Menegatti, A. Zanella, S. Zilli, F. Zorzi, and E. Pagello, "Range-only SLAM with a mobile robot and a wireless sensor networks," in *Proc. IEEE Int. Conf. Robot. Autom.*, May 2009, pp. 8–14.

[5] J.-L. Blanco, J. Gonzalez, and J.-A. Fernandez-Madrigal, "A pure probabilistic approach to range-only SLAM," in *Proc. IEEE Int. Conf. Robot. Autom.*, May 2008, pp. 1436–1441.

[6] S. Shue, N. Shetty, A. Browne, J. Conrad, and A. Leo, "Particle filter approach to utilization of wireless signal strength for mobile robot localization in indoor environments," *Int. J. Wireless Mobile Netw.*, vol. 10, p. 18, Aug. 2018.

[7] J. Kim and D. Kim, "Cooperative range-only SLAM based on Rao-Blackwellized particle filter," in *Proc. IEEE Sensors*, Oct. 2019, pp. 1–4.

[8] J.-L. Blanco, J. González, and J.-A. Fernández-Madrigal, "Optimal filtering for non-parametric observation models: Applications to localization and SLAM," *Int. J. Robot. Res.*, vol. 29, no. 14, pp. 1726–1742, Dec. 2010, doi: 10.1177/0278364910364165.

[9] A. Sato, M. Nakajima, and N. Kohtake, "Rapid BLE beacon localization with range-only EKF-SLAM using beacon interval constraint," in *Proc. Int. Conf. Indoor Positioning Indoor Navigat. (IPIN)*, Sep. 2019, pp. 1–8.

[10] A. Torres-Gonzalez, J. R. M.-D. Dios, and A. Ollero, "Efficient robot-sensor network distributed SEIF range-only SLAM," in *Proc. IEEE Int. Conf. Robot. Autom. (ICRA)*, May 2014, pp. 1319–1326.

[11] F. Herranz, A. Llamazares, E. Molinos, and M. Ocana, "A comparison of SLAM algorithms with range only sensors," in *Proc. IEEE Int. Conf. Robot. Autom. (ICRA)*, May 2014, pp. 4606–4611.

[12] J. Huang, D. Millman, M. Quigley, D. Stavens, S. Thrun, and A. Aggarwal, "Efficient, generalized indoor WiFi GraphSLAM," in *Proc. IEEE Int. Conf. Robot. Autom.*, May 2011, pp. 1038–1043.

[13] B. Boots and G. Gordon, "A spectral learning approach to range-only SLAM," in *Proc. 30th Int. Conf. Mach. Learn.*, Atlanta, GA, USA, Jun. 2013, vol. 28, no. 1, pp. 19–26.

[14] J. J. Leonard, R. J. Rikoski, P. M. Newman, and M. Bosse, "Mapping partially observable features from multiple uncertain vantage points," *Int. J. Robot. Res.*, vol. 21, nos. 10–11, pp. 943–975, Oct. 2002.

[15] E. Olson, J. J. Leonard, and S. Teller, "Robust range-only beacon localization," *IEEE J. Ocean. Eng.*, vol. 31, no. 4, pp. 949–958, Oct. 2006.

[16] Y. Zhou, "An efficient least-squares trilateration algorithm for mobile robot localization," in *Proc. IEEE/RSJ Int. Conf. Intell. Robot. Syst.*, Oct. 2009, pp. 3474–3479.

[17] F. Caballero, L. Merino, and A. Ollero, "A general Gaussian-mixture approach for range-only mapping using multiple hypotheses," in *Proc. IEEE Int. Conf. Robot. Autom.*, May 2010, pp. 4404–4409.

[18] F. R. Fabresse, F. Caballero, I. Maza, and A. Ollero, "An efficient approach for undelayed range-only SLAM based on Gaussian mixtures expectation," *Robot. Auto. Syst.*, vol. 104, pp. 40–55, Jun. 2018.

[19] J. Djugash and S. Singh, "A robust method of localization and mapping using only range," in *Proc. Experim. Robot.*, 2009, pp. 341–351.

[20] M. Montemerlo, S. Thrun, D. Koller, and B. Wegbreit, "FastSLAM: A factored solution to the simultaneous localization and mapping problem," in *AAAI Conf. Artif. Intell.*, Nov. 2002, pp. 593–598.

[21] D. Sun, A. Kleiner, and T. M. Wendt, "Multi-robot range-only slam by active sensor nodes for urban search and rescue," in *Robot Soccer World Cup XII*, L. Iocchi, H. Matsubara, A. Weitzenfeld, and C. Zhou, Eds. Berlin, Germany: Springer-Verlag, 2009, pp. 318–330.

[22] S. Marano, W. Gifford, H. Wymeersch, and M. Win, "NLOS identification and mitigation for localization based on UWB experimental data," *IEEE J. Sel. Areas Commun.*, vol. 28, no. 7, pp. 1026–1035, Sep. 2010.

[23] D. Dardari, A. Conti, U. Ferner, A. Giorgetti, and M. Z. Win, "Ranging with ultrawide bandwidth signals in multipath environments," *Proc. IEEE*, vol. 97, no. 2, pp. 404–426, Feb. 2009.

[24] J. D. Hol, F. Dijkstra, H. Luinge, and T. B. Schon, "Tightly coupled UWB/IMU pose estimation," in *Proc. IEEE Int. Conf. Ultra-Wideband*, Sep. 2009, pp. 688–692.

[25] F. R. Fabresse, F. Caballero, I. Maza, and A. Ollero, "Robust range-only SLAM for unmanned aerial systems," *J. Intell. Robot. Syst.*, vol. 84, nos. 1–4, pp. 297–310, Dec. 2015.

[26] A. Rosales, G. Scaglia, V. Mut, and F. di Sciascio, "Formation control and trajectory tracking of mobile robotic systems—A Linear Algebra approach," *Robotica*, vol. 29, no. 3, p. 335–349, 2011.

[27] J. Wang and Y. Takahashi, "SLAM method based on independent particle filters for landmark mapping and localization for mobile robot based on HF-band RFID system," *J. Intell. Robot. Syst.*, vol. 92, nos. 3–4, pp. 413–433, Dec. 2018.

[28] J.-H. Kim and D. Kim, "Cooperative range-only SLAM based on sum of Gaussian filter in dynamic environments," in *Proc. IEEE/RSJ Int. Conf. Intell. Robot. Syst. (IROS)*, Nov. 2019, pp. 2139–2144.

[29] J. Djugash, S. Singh, G. Kantor, and W. Zhang, "Range-only SLAM for robots operating cooperatively with sensor networks," in *Proc. IEEE Int. Conf. Robot. Autom. (ICRA)*, Oct. 2006, pp. 2078–2084.

[30] F. R. Fabresse, F. Caballero, and A. Ollero, "Decentralized simultaneous localization and mapping for multiple aerial vehicles using range-only sensors," in *Proc. IEEE Int. Conf. Robot. Autom. (ICRA)*, May 2015, pp. 6408–6414.

[31] W. Zhen and S. Scherer, "Estimating the localizability in tunnel-like environments using LiDAR and UWB," in *Proc. Int. Conf. Robot. Autom. (ICRA)*, May 2019, pp. 4903–4908.

[32] K. Li, C. Wang, S. Huang, G. Liang, X. Wu, and Y. Liao, "Self-positioning for UAV indoor navigation based on 3D laser scanner, UWB and INS," in *Proc. IEEE Int. Conf. Inf. Autom. (ICIA)*, Aug. 2016, pp. 498–503.

[33] Y. Song, M. Guan, W. P. Tay, C. L. Law, and C. Wen, "UWB/LiDAR fusion for cooperative range-only SLAM," in *Proc. Int. Conf. Robot. Autom. (ICRA)*, May 2019, pp. 6568–6574.

[34] F. J. Perez-Grau, F. Caballero, L. Merino, and A. Viguria, "Multi-modal mapping and localization of unmanned aerial robots based on ultra-wideband and RGB-D sensing," in *Proc. IEEE/RSJ Int. Conf. Intell. Robot. Syst. (IROS)*, Sep. 2017, pp. 3495–3502.
[35] P. Lutz, M. J. Schuster, and F. Steidle, "Visual-inertial SLAM aided estimation of anchor poses and sensor error model parameters of UWB radio modules," in *Proc. 19th Int. Conf. Adv. Robot. (ICAR)*, Dec. 2019, pp. 739–746.
[36] C. Wang, H. Zhang, T.-M. Nguyen, and L. Xie, "Ultra-wideband aided fast localization and mapping system," in *Proc. IEEE/RSJ Int. Conf. Intell. Robot. Syst. (IROS)*, Sep. 2017, pp. 1602–1609.

Jun Wang received the B.S. degree from the Beijing Information Science and Technology University, Beijing, China, in 2013, and the master's and Ph.D. degrees with the Department of Human and Artificial Intelligent Systems, University of Fukui, Fukui, Japan, in 2016 and 2019, respectively.

He currently joined the Department of Precision Instrument, Tsinghua University, Beijing, as a Postdoc. His research interests include state estimation, SLAM, particle filter, sensor fusion, and applied robotics.

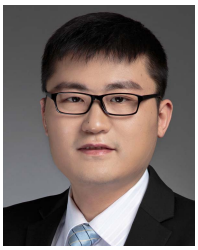

Ziyang Meng (Senior Member, IEEE) received the B.S. degree (Hons.) from the Huazhong University of Science and Technology, Wuhan, China, in 2006, and the Ph.D. degree from Tsinghua University, Beijing, China, in 2010.

He was an exchange Ph.D. Student with Utah State University, Logan, UT, USA, from 2008 to 2009. Prior to joining Tsinghua University, he held Postdoc, Researcher, and Humboldt Research Fellow positions at, Shanghai Jiao Tong University, Shanghai, China, KTH Royal Institute of Technology, Stockholm, Sweden, and Technical University of Munich, Munich, Germany, respectively from 2010 to 2015. He is currently an Associate Professor with the Department of Precision Instrument, Tsinghua University. His research interests include distributed control and optimization, space science, and intelligent navigation technique.

Dr. Meng serves as an Associate Editors for *Systems & Control Letters* and *IET Control Theory & Applications*.

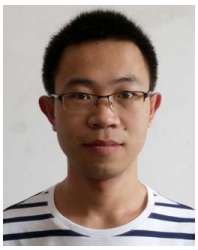

Lei Wang received the B.S. degree from Wuhan University, Wuhan, China, in 2016. He is currently pursuing the Ph.D. degree with the Department of Precision Instrument, Tsinghua University, Beijing. China.

His research interests include state estimation, cooperative localization, and distributed control.